SUPPLEMENTAL INFORMATION

Supplemental Table 1 – Amino acid residues and the corresponding transmembrane helices found within 4.5 Å of the highest affinity docking poses of Verapamil and Daunorubicin in the starting wide open to the cytoplasm conformation of P-glycoprotein. The table lists contacts for each of the six independent simulations. Lists were compiled after the respective P-glycoprotein, lipid, water and drug systems had been independently heated and equilibrated at 310 K. Helix "0" indicates contacts outside of the transmembrane region of the protein. TM helices were the same as listed in the Uniprot database (http://www.uniprot.org/uniprot/P08183). Residues that have been experimentally determined to contribute to transport drug binding are identified in the respective columns. Numbers refer to the following experimental works with residue numbers for human P-gp:

1) Loo, T. W., Bartlett, M. C., and Clarke, D. M. (2009) Identification of residues in the drug translocation pathway of the human multidrug resistance P-glycoprotein by arginine mutagenesis, J Biol Chem 284, 24074-24087;
2) Li, J., Jaimes, K. F., and Aller, S. G. (2014) Refined structures of mouse P-glycoprotein, Protein Sci 23, 34-46;
3) Loo, T. W., and Clarke, D. M. (2005) Do drug substrates enter the common drug-binding pocket of P-glycoprotein through "gates"?, Biochem Biophys Res Commun 329, 419-422;
4) Loo, T. W., Bartlett, M. C., and Clarke, D. M. (2006) Transmembrane segment 1 of human P-glycoprotein contributes to the drug-binding pocket, Biochem J 396, 537-545;

5) Loo, T. W., Bartlett, M. C., and Clarke, D. M. (2006) Transmembrane segment 7 of human P-glycoprotein forms part of the drug-binding pocket, Biochem J 399, 351-359;

6) Loo, T. W., Bartlett, M. C., and Clarke, D. M. (2007) Suppressor mutations in the transmembrane segments of P-glycoprotein promote maturation of processing mutants and disrupt a subset of drug-binding sites, J Biol Chem 282, 32043-32052.

7) Loo, T. W., Bartlett, M. C., and Clarke, D. M. (2008) Arginines in the first transmembrane segment promote maturation of a P-glycoprotein processing mutant by hydrogen bond interactions with tyrosines in transmembrane segment 11, J Biol Chem 283, 24860-24870;

8) Loo, T. W., and Clarke, D. M. (2013) Drug rescue distinguishes between different structural models of human P-glycoprotein, Biochemistry 52, 7167-7169.

Computationally observed daunorubicin binding sites:

9) Ma, J., and Biggin, P. C. (2013) Substrate versus inhibitor dynamics of P-glycoprotein, Proteins 81, 1653-1668.

Dauno-rubicin 1	resname	resid	TM-helix	AA-type	Exp't-ally ID'd	Vera-pamil 1	resname	resid	TM-helix	AA-type	Exp't-ally ID'd
	HIS	61	1	basic	7		TRP	232	4	aromatic	
	LEU	65	1	nonpolar	2,4,7		ILE	299	5	nonpolar	
	ALA	129	2	nonpolar			ALA	302	5	nonpolar	1,8
	GLN	132	2	polar			PHE	303	5	aromatic	2
	VAL	133	2	nonpolar			ILE	306	5	nonpolar	3,5
	ASP	188	3	acidic			TYR	307	5	aromatic	2
	LYS	189	3	basic			TYR	310	5	aromatic	2
	MET	192	3	nonpolar			PHE	336	6	aromatic	2,9
	GLN	195	3	polar			PHE	343	6	aromatic	2,3, 5,6
	GLN	347	6	polar			GLN	725	7	polar	2
	PHE	942	11	aromatic	1,3,9		PRO	726	7	nonpolar	
	GLN	946	11	polar	1		PHE	728	7	aromatic	2,5
	TYR	950	11	aromatic			ALA	729	7	nonpolar	
							PHE	732	7	aromatic	2
							PHE	770	8	aromatic	2
							SER	979	12	polar	
							VAL	982	12	nonpolar	3,9
							PHE	983	12	aromatic	2
							MET	986	12	nonpolar	2
							GLN	990	12	polar	2,9

Dauno-rubicin 2	resname	resid	TM-helix	AA-type	Exp't-ally ID'd	Vera-pamil 2	resname	resid	TM-helix	AA-type	Exp't-ally ID'd
	HIS	61	1	basic	7		TRP	232	4	aromatic	
	LEU	65	1	nonpolar	2,4,7		ILE	299	5	nonpolar	2
	VAL	125	2	nonpolar			ALA	302	5	nonpolar	1,8
	ALA	129	2	nonpolar			PHE	303	5	aromatic	2
	GLN	132	2	polar			ILE	306	5	nonpolar	3,5
	VAL	133	2	nonpolar			TYR	310	5	aromatic	2
	ASP	188	3	acidic			PHE	336	6	aromatic	2,9
	MET	192	3	nonpolar			LEU	339	6	nonpolar	1,3,9
	GLN	195	3	polar			ILE	340	6	nonpolar	2,3
	GLN	347	6	polar			PHE	343	6	aromatic	2,3, 5,6
	GLU	875	0	acidic			PHE	728	7	aromatic	2,5
	MET	876	0	nonpolar			PHE	770	8	aromatic	2
	LEU	879	0	nonpolar			VAL	982	12	nonpolar	3,9
	PHE	938	11	aromatic			MET	986	12	nonpolar	2
	PHE	942	11	aromatic	1,3,9		GLN	990	12	polar	2,9
	GLN	946	11	polar	1		SER	993	12	polar	1
	MET	949	11	nonpolar	2,9		PHE	994	12	aromatic	
	TYR	950	11	aromatic							

Dauno-rubicin 3	resname	resid	TM-helix	AA-type	Exp't-ally ID'd	Vera-pamil 3	resname	resid	TM-helix	AA-type	Exp't-ally ID'd
	HIS	61	1	basic	7		TRP	232	4	aromatic	
	LEU	65	1	nonpolar	2,4,7		ILE	299	5	nonpolar	2
	ALA	129	2	nonpolar			ALA	302	5	nonpolar	1,8
	GLN	132	2	polar			PHE	303	5	aromatic	2,9
	VAL	133	2	nonpolar			ILE	306	5	nonpolar	3,5
	MET	192	3	nonpolar			TYR	307	5	aromatic	2
	GLN	195	3	polar			TYR	310	5	aromatic	2
	GLN	347	6	polar			PHE	336	6	aromatic	2,9
	PRO	350	6	nonpolar			ILE	340	6	nonpolar	2,3
	GLU	875	0	acidic			PHE	343	6	aromatic	2,3, 5,6
	PHE	942	11	aromatic	1,3,9		PHE	728	7	aromatic	2,5
	SER	943	11	polar			PHE	732	7	aromatic	2
	GLN	946	11	polar	1		VAL	982	12	nonpolar	3,9
	MET	949	11	nonpolar	2,9		PHE	983	12	aromatic	2
	TYR	950	11	aromatic			ALA	985	12	nonpolar	3,9
							MET	986	12	nonpolar	2
							GLY	989	12	nonpolar	
							GLN	990	12	polar	2,9
							PHE	994	12	aromatic	

Dauno-rubicin 4	resname	resid	TM-helix	AA-type	Exp't-ally ID'd	Vera-pamil 4	resname	resid	TM-helix	AA-type	Exp't-ally ID'd
	HIS	61	1	basic	7		LEU	225	4	nonpolar	
	ALA	129	2	nonpolar			TRP	232	4	aromatic	
	GLN	132	2	polar			ILE	299	5	nonpolar	2
	VAL	133	2	nonpolar			ALA	302	5	nonpolar	1,8
	MET	192	3	nonpolar			PHE	303	5	aromatic	2,9
	GLN	195	3	polar			ILE	306	5	nonpolar	3,5
	GLN	347	6	polar			TYR	307	5	aromatic	2
	GLU	875	0	acidic			TYR	310	5	aromatic	2
	MET	876	0	nonpolar			PHE	336	6	aromatic	2,9
	PHE	938	11	aromatic			PHE	343	6	aromatic	2,3, 5,6
	PHE	942	11	aromatic	1,3,9		PHE	728	7	aromatic	2,5
	GLN	946	11	polar	1		PHE	732	7	aromatic	2
	MET	986	12	nonpolar	2		VAL	982	12	nonpolar	3,9
							PHE	983	12	aromatic	3
							MET	986	12	nonpolar	2
							GLN	990	12	polar	2,9
							PHE	994	12	aromatic	

Dauno-rubicin 5	resname	resid	TM-helix	AA-type	Exp't-ally ID'd	Vera-pamil 5	resname	resid	TM-helix	AA-type	Exp't-ally ID'd
	HIS	61	1	basic	7		TRP	232	4	aromatic	
	LEU	65	1	nonpolar	2,4,7		ILE	299	5	nonpolar	2
	ALA	129	2	nonpolar			ALA	302	5	nonpolar	1,8
	GLN	132	2	polar			PHE	303	5	aromatic	2,9
	VAL	133	2	nonpolar			ILE	306	5	nonpolar	3,5
	ASP	188	3	acidic			TYR	307	5	aromatic	2
	MET	192	3	nonpolar			TYR	310	5	aromatic	2
	GLN	195	3	polar			PHE	336	6	aromatic	2,9
	GLN	347	6	polar			LEU	339	6	nonpolar	1,3,9
	GLU	875	0	acidic			PHE	343	6	aromatic	2,3, 5,6
	PHE	938	11	aromatic			GLN	725	7	polar	2
	PHE	942	11	aromatic	1,3,9		PHE	728	7	aromatic	2,5
	GLN	946	11	polar	1		PHE	732	7	aromatic	2
	MET	949	11	nonpolar	2		PHE	770	8	aromatic	2
	TYR	950	11	aromatic			GLN	838	9	polar	
							MET	986	12	nonpolar	2
							GLN	990	12	polar	2,9
							PHE	994	12	aromatic	

Dauno-rubicin 6	resname	resid	TM-helix	AA-type	Exp't-ally ID'd	Vera-pamil 6	resname	resid	TM-helix	AA-type	Exp't-ally ID'd
	HIS	61	1	basic	7		TRP	232	4	aromatic	
	LEU	65	1	nonpolar	2,4,7		ILE	299	5	nonpolar	2
	ALA	129	2	nonpolar			ALA	302	5	nonpolar	1,8
	LYS	189	3	basic			PHE	303	5	aromatic	2,9
	MET	192	3	nonpolar			TYR	307	5	aromatic	2
	GLN	195	3	polar			PHE	336	6	aromatic	2,9
	GLN	347	6	polar			GLN	725	7	polar	2
	GLU	875	0	acidic			PRO	726	7	nonpolar	
	MET	876	0	nonpolar			PHE	728	7	aromatic	2,5
	PHE	942	11	aromatic	1,3,9		ALA	729	7	nonpolar	
	THR	945	11	polar	3		PHE	732	7	aromatic	2
	GLN	946	11	polar	1		PHE	770	8	aromatic	2
							SER	979	12	polar	
							VAL	982	12	nonpolar	3,9
							PHE	983	12	aromatic	2
							MET	986	12	nonpolar	2
							GLN	990	12	polar	2,9
							SER	993	12	polar	1
							PHE	994	12	aromatic	

Supplemental Table II. Amino acid residues found to be within 4.5 Å of tariquidar docked at the three tariquidar sites described in the text and Figure 4.

Site 1:
T240, E243, L244, Y247, A248, A250, G251, A252, A254, E255, L281, K285, K291, T785, R789, T815, L818, A819, A822, A823, N824, K826, G827, G830, D997

Site 2:
W232, A292, N296, I299, F303, A718, N721, G722, Q725, F770, Q773, G774, F777, G778, G781, A823, K826, G827, G830, S831, L833, A834, T837, Q838, M986, Q990, F994, N997

Site 3:

M69, F72, F303, Y307, Y310, F314, T333, F336, S337, I340, F728, F732, V865, I868, A869, G872, V873, M949, S952, Y953, F978, V981, V982, G984, A985, M986, V988

Supplemental Figure 1. Human P-glycoprotein conformations extracted from TMD simulations at the indicated molecular dynamics target. The top row shows human P-gp models at the four indicated target structures. The bottom row shows the equivalent structures rotated about the Y-axis by 90°. Human P-gp was pushed to each structure in TMD simulations as described in [32] and Methods. Each structure shown has calculated RMSD values for the targeted Cα atoms of < 0.3 Å. The indicated targets were mouse P-gp (4KSB)[28], lipid flippase MsbA (3B5X)[19], bacterial *Sav*1866 (2HYD)[22], and the transition state MsbA structure (3B5Z)[19].

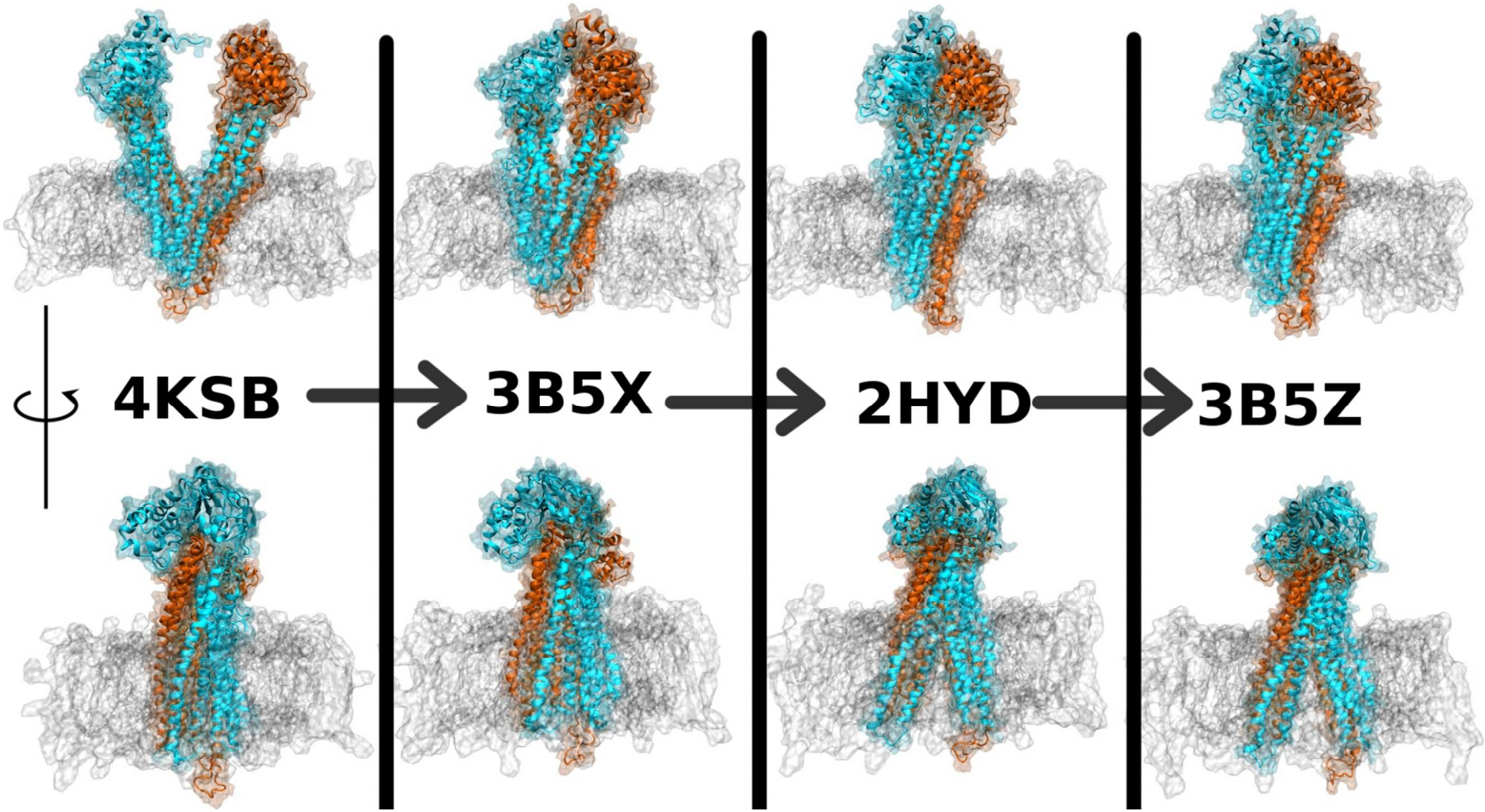

Supplemental Figure 2. Dynamics of drug transport through P-glycoprotein: Daunorubicin movement. The figure shows an animation of Daunorubicin moving through the membrane during the targeted molecular dynamics simulations described in the text.

Supplemental Figure 3. Dynamics of drug transport through P-glycoprotein: Verapamil movement. The figure shows an animation of Verapamil moving through the membrane during the targeted molecular dynamics simulations described in the text.

Supplemental Figure 4. Movement of Daunorubicin and Verapamil through P-glycoprotein when positioned at non-optimal starting locations within the drug binding sites. Docking of daunorubicin and verapamil was performed as described in the text. Panel A shows the average movement of daunorubicin during a simulated catalytic cycle (squares – daunorubicin starting at the putative R site – data reproduced from Figure 3; triangles – daunorubicin at the putative H site). Panel B shows the average movement of verapamil (squares – starting at the putative H site – data reproduced from Figure 3; triangles – starting at the putative R site). Panel C shows the variability observed in the individual runs made with verapamil starting at the putative R site.

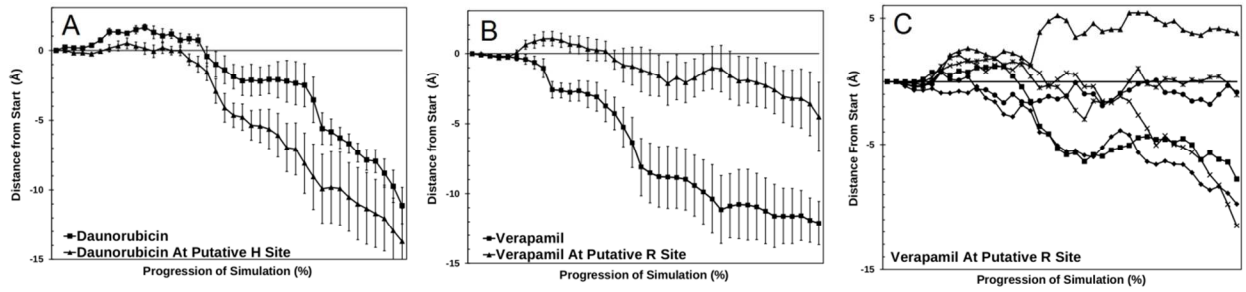

Supplemental Figure 5. Movement of Daunorubicin through P-gp for all six simulations. Results are similar to those shown in Figure 5 except that the results from each individual simulation are presented. Each panel shows 3D plots of the numbers of contacts of the transmembrane helices of P-gp that were within 4.5Å of Daunorubicin during the six independent simulations versus the progress of the TMD experiment given in percent completion. Helices 0 through 12 represent the 12 membrane helices of P-gp (labeled 1-12) while "0" represents any contact with Daunorubicin outside of the 12 TMs. The individual simulations are plotted separately and are labeled "Daunorubicin 1" through "Daunorubicin 6".

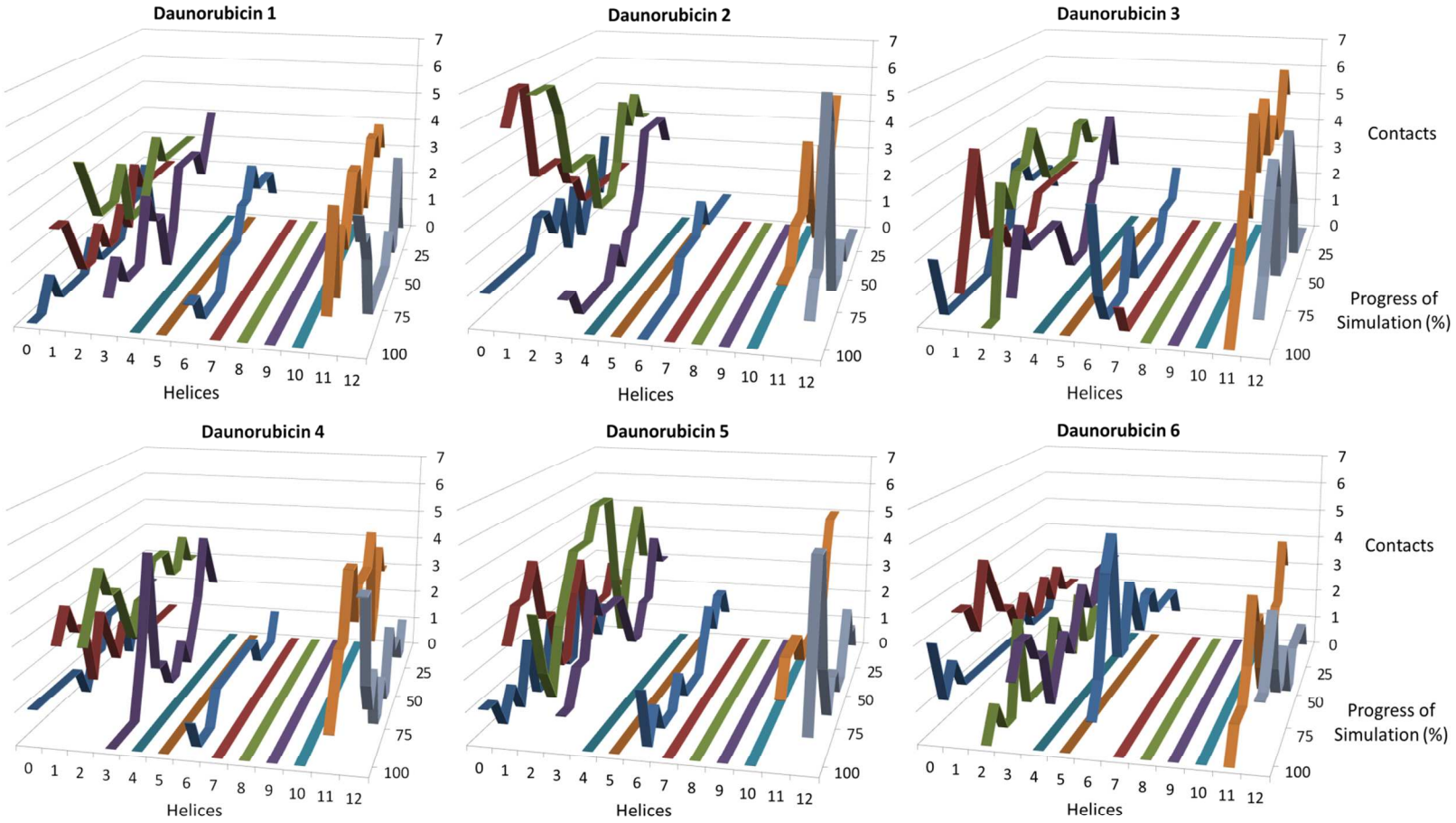

Supplemental Figure 6. Movement of Verapamil through P-gp for all six simulations. Results are similar to those shown in Supplemental Figure 5 except that the results from each of the individual simulations with Verapamil are presented.

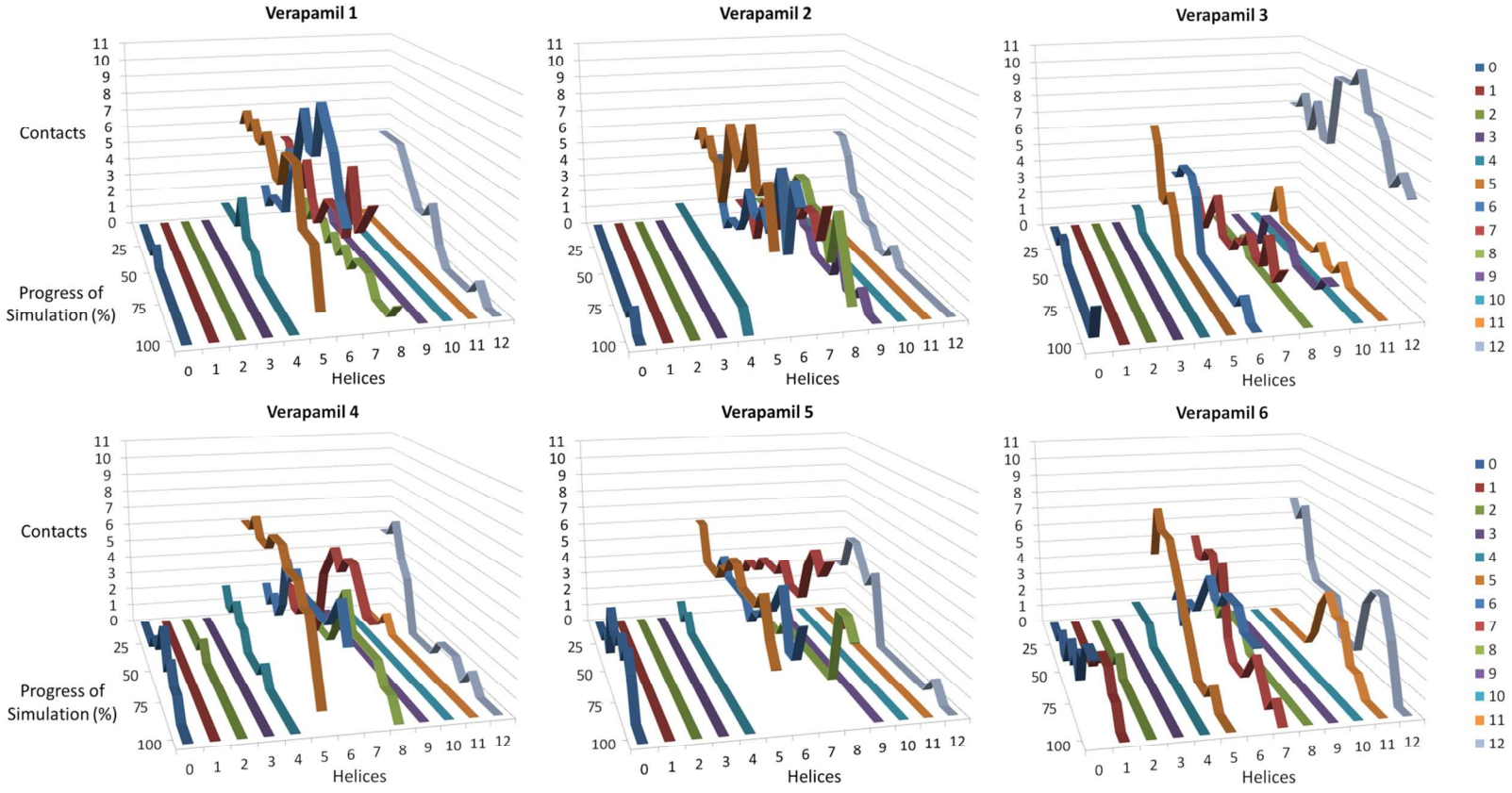

Supplemental Figure 7. Interactions between P-gp and Daunorubicin (left) or Verapamil (right) with acidic (top) or basic (bottom) residues of the transmembrane helices. Averages of the contacts for all six simulations are presented.

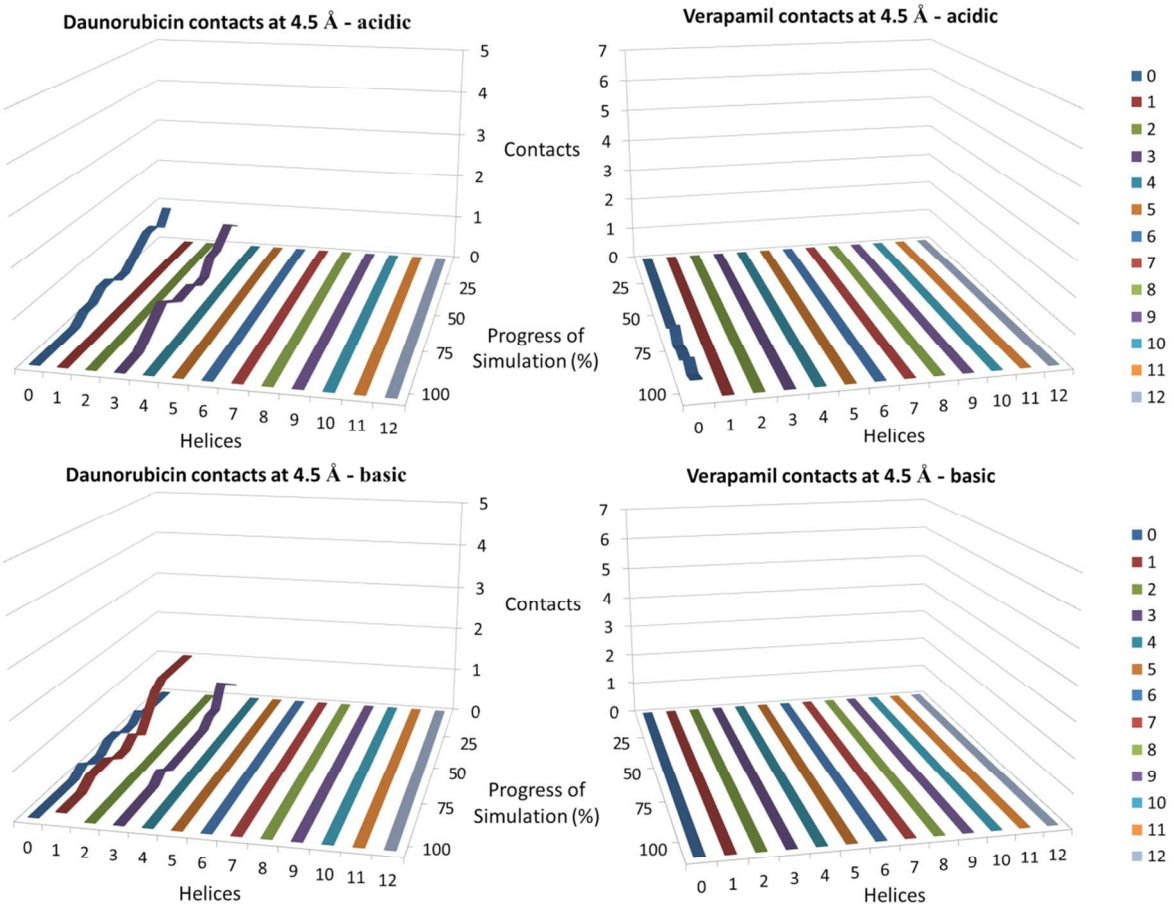

Supplemental Figure 8. RMSD changes for Daunorubicin and Verapamil during targeted molecular dynamics simulations. The movement of either Daunorubicin (simulation 6) or Verapamil (simulation 6) was plotted as the respective root mean squared deviation (RMSD, in Å) versus the progress of the simulation.